Nanoparticle-polymer-composite volume gratings incorporating chain-transfer agents for holography and slow-neutron optics

Ryuta Fujii,[1] Jinxin Guo,[1] Jürgen Klepp,[2] Christian Pruner,[3] Martin Fally,[2] and Yasuo Tomita[1,*]

[1] *Department of Engineering Science, University of Electro-Communications, 1-5-1 Chofugaoka, Chofu, Tokyo 182-8585, Japan*

[2] *Faculty of Physics, University of Vienna, Boltzmanngasse 5, A-1090 Vienna, Austria*

[3] *Department of Materials Science and Physics, University of Salzburg, A-5020 Salzburg, Austria*

[*] *Corresponding author: ytomita@uec.ac.jp*

Compiled April 25, 2014

We demonstrate two-fold enhancement of the saturated refractive-index modulation (Δn_{sat}) recorded in a photopolymerizable nanoparticle-acrylate polymer composite film by incorporating thiols acting as chain-transfer agents. The chain-transfer reaction of thiols with acrylate monomer reduces the polymer crosslinking density and facilitates the mutual diffusion of nanoparticles and monomer during holographic exposure. These modifications provide increased density modulations of nanoparticles and the formed polymers, resulting in the enhancement of Δn_{sat} as high as 1.6×10^{-2} at a wavelength of 532 nm. The incorporation of thiols also leads to shrinkage suppression and to improvement of the grating's spatial frequency response. Such simultaneous improvement is very useful for holographic applications in light and neutron optics.

OCIS codes: (090.7330) Volume holographic gratings; (160.4236) Nanomaterials; (160.5470) Polymers.

All-organic holographic photopolymers and polymer-dispersed liquid crystals (HPDLCs) have been extensively investigated for their uses in photonics and information display so far [1–3]. Since 2002 organic-inorganic holographic nanocomposite materials, the so-called photopolymerizable nanoparticle-polymer composites (NPCs), have been studied extensively. They consist of inorganic (such as TiO_2, SiO_2, ZrO_2, $LaPO_4$ and nanozeolites) nanoparticles that are uniformly dispersed in host monomer capable of radical-mediated photopolymerization [4–9]. The statistical thermodynamic interaction between monomer and nanoparticles facilitates the polymerization-driven mutual diffusion process during holographic exposure. This leads to light-induced redistribution of the formed polymer and nanoparticles in the bright and dark regions of a light pattern, respectively. As a result, the formed spatial distribution of dispersed nanoparticles is out of phase with respect to a holographically exposed light pattern. This technique, the so-called holographic assembly of nanoparticles in photopolymer [10], enables us to perform the single step formation of large scale photonic lattice structures. When a combination of monomer and nanoparticles having a large difference in their refractive indices is chosen appropriately, the saturated refractive index modulation (Δn_{sat}) of volume gratings recorded in NPCs can be as high as $\sim 8\times10^{-3}$ at a wavelength of 532 nm [5, 6]. The mechanical and thermal stability of recorded volume gratings against polymerization shrinkage and thermal changes in film thickness and refractive index can also be improved [11,12]. Versatile applications of NPCs have been reported so far because they can be tailored. These include holographic data storage [13], distributed feedback lasers [14,15], nonlinear optics [16] and holographic diffractive elements for slow-neutron (cold and very cold neutron) beam control [17–19].

Generally, NPC volume gratings with large Δn_{sat} at short grating spacing (*i.e.*, high spatial frequencies) and with low distortion are desired for light and slow-neutron optics applications. In particular, a slow-neutron mirror near 100% reflectivity requires the use of (meth)acrylate-based NPC volume gratings possessing large neutron refractive index modulation (Δn_{neu}) [17, 18], moderate film thickness and short grating spacing. Here, Δn_{neu} is given by $\lambda_n^2 b_c \Delta\rho/2\pi$, where λ_n is a neutron wavelength, b_c the coherent scattering length for a particular isotope of an atom in a dispersed nanoparticle (*e.g.*, ZrO_2 and SiO_2 nanoparticles used for slow-neutron diffraction [17–19]) and $\Delta\rho$ the modulation amplitude of the atomic number density (*i.e.*, the volume modulation amplitude of nanoparticles between the bright and the dark fringe regions). The first requirement of large Δn_{neu} can be translated into large Δn_{sat} since $\Delta\rho$ is approximately given by $2\Delta n_{sat}/|n_n - n_p|$, where n_n and n_p are refractive indices of a nanoparticle and the formed polymer, respectively [4]. The second requirement of moderate film thickness stems from the fact that the diffraction from a highly angle-selective very thick volume grating results in reduced neutron diffraction efficiencies due to averaging of diffracted beam power from a neutron beam with limited beam collimation [17]. The third requirement of short grating spacing is to obtain large Klein-Cook parameter Q that is proportional to film thickness and is inversely proportional to the grating spacing squared [17]. Thus, Q can be increased by use of short grating spacing even for a moderately thick volume grating.

These requirements particularly for slow-neutron optics applications need simultaneous improvement of the following common problems encountered in photopolymer volume gratings: a reduction of Δn_{sat} in high spa-

tial frequency regions and the grating-fidelity degradation due to polymerization shrinkage. The former takes place due to the non-local photopolymerization response [20] caused by the rapid growth of crosslinking polymer chains penetrating into the dark fringe regions and to the phase separation/flocculation phenomena in multi-component holographic photopolymers including HPDLCs [21] and NPCs. The latter can be obviated substantively by chemical modifications of photopolymerizations as well as by nanoparticle dispersion. Therefore, it is necessary to 1) facilitate the mutual diffusion of monomer and nanoparticles during holographic exposure, 2) minimize the non-local response, and 3) avoid the rapid formation of high molecular-weight polymer that leads to noticeable bulk shrinkage. These may be achieved by suppression of rapidly crosslinking polymer networks in free radical-mediated chain-growth polymerizations.

In this Letter we report a method of noticeable improvement of the volume grating properties by chemical modification of the photopolymerization process in NPCs based on free radical-mediated chain-growth (meth)acrylate polymerizations. This modification can be performed by introducing the chain-transfer reaction mechanism [22–24]. For (meth)acrylate monomers light absorption by a photosensitizer generates primary radicals, followed by generation of monomer radicals during the reaction between primary radical and monomer and by the termination of propagating monomer-radical chains. On the other hand, the chain-transfer reaction process includes the premature termination of propagating monomer-radical chains [22]; doped chain-transfer agents such as thiols cause a chain breaking mechanism in which the radical formed through the transfer serves as a new initiation site [25], as shown below.

$$\mathrm{M_n}\cdot + \mathrm{XA} \longrightarrow \mathrm{M}_n - \mathrm{X} + \mathrm{A}\cdot \qquad \text{(Chain-transfer)}$$
$$\mathrm{A}\cdot + \mathrm{M} \longrightarrow \mathrm{M}_1\cdot \qquad \text{(Reinitiation)}$$

where $\mathrm{M_n}$ ($\mathrm{M_n}\cdot$) is an n monomer-chain unit (a propagating radical of an n monomer-chain unit), XA a chain-transfer agent that may be monomer or initiator or other substances, and X species transferred. The crosslinking density of the formed polymer may be controlled by the doping concentration and the functionality of chain-transfer agents because of this chain-breaking reaction.

In the sample preparation surface-modified ZrO_2 nanoparticles with an average core size of 3 nm were prepared by liquid-phase synthesis and dissolved in toluene solution [6]. The ZrO_2 nanoparticle sol was dispersed to multifunctional acrylate monomer, 2-propenoic acid, (octahydro-4,7-methano-1H-indene-2,5-diyl)bis(methylene) ester (A-DCP, Shin-Nakamura Chemical Co. Ltd.). We used titanocene (Irgacure784, Ciba) as a radical photo-initiator providing the photosensitivity at wavelengths shorter than 550 nm. The concentration of the initiator was 1 wt.% with respect to the acrylate monomer. We also added single functional mono-thiol, methyl-3-mercaptopropionate (M1434, Tokyo Chemical Industry Co. Ltd.), as a chain-transfer agent. The chemical structures of the acrylate and the mono-thiol monomers are shown in Fig. 1. Such mixture was cast on a 10-μm-spacer loaded glass plate and was dried to remove toluene. Finally, it was covered with another glass plate to be used as a film sample dispersed with 35 vol.% of ZrO_2 nanoparticles (the optimum nanoparticle concentration maximizing Δn_{sat}) [6].

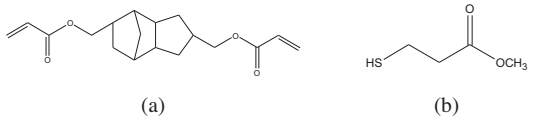

(a) (b)

Fig. 1. Chemical structures of (a) acrylate and (b) mono-thiol monomers.

In order to investigate the doping effect of chain-transferring thiol on the photopolymerization kinetics, the photo-differential scanning calorimetry (photo-DSC) was performed. The photo-DSC measurement gave time-dependent conversion and photo-induced polymerization rate (R_p) of the monomer-thiol mixture in real time [12]. We employed a commercially available photo-calorimeter (Q200, TA instrument) equipped with a refrigerated cooling system (RCS90, TA instrument) in order to accurately maintain the isotherm condition at 25° C [12]. Polymerizations were initiated by a loosely focused light beam via a lightguide that was connected to a high-pressure mercury arc lamp (SUPER CURE-204S, SAN-EI) through a 532-nm bandpass filter. The curing intensity was set to be 50 mW/cm^2 at a wavelength of 532 nm used in our holographic measurement (see below).

In the holographic recording experiment we used an uncured film sample to record an unslanted plane-wave transmission grating at a recording intensity of 50 mW/cm^2 from a frequency-doubled Nd:YVO_4 laser operating at a wavelength of 532 nm. A low intensity He-Ne laser beam operating at a wavelength of 633 nm that was insensitive to the employed radical photo-initiator was employed as a Bragg-matched readout beam to monitor the grating buildup dynamics. All the beams were s-polarized. We measured the diffraction efficiency (η) that was defined as the ratio of the 1st-order diffracted signal to the sum of the 0th- and 1st-order signals. The effective thickness (ℓ) of each sample was estimated from a least-squares curve fit to the Bragg-angle detuning data of the saturated η (η_{sat}) with a coupled-wave approach using the beta-value method (Uchida's formalism) for an unslanted transmission grating [26]. Then, Δn_{sat} was extracted from η_{sat} with the help of the above formula and ℓ. Note that the refractive index modulation (Δn) of a volume grating being recorded at 633 nm was converted to that at 532 nm. We also evaluated the out-of-plane fractional thickness change (σ) of a recorded film sample due to polymerization shrinkage by means of Dhar *et al.*'s holographic method [27].

Figure 2 shows temporal traces of conversions of the

monomer-thiol mixtures at various mono-thiol concentrations. The molar concentration is with respect to the acrylate monomer. It can be seen that while the final conversion of the neat monomer is approximately 0.59, typical for highly crosslinking (meth)acrylate monomers, those of the monomer-thiol mixtures increases with increasing doping concentrations of mono-thiols up to 0.75. This result indeed indicates that mono-thiols react with propagating acrylate monomer radicals and terminate the free radical-mediated chain-growth polymerizations via the chain-transfer mechanism.

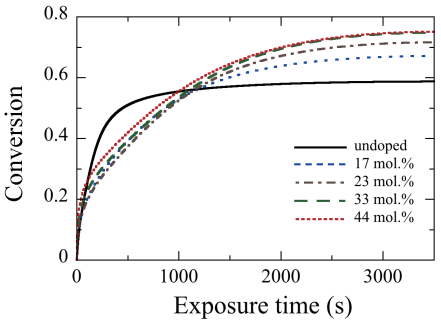

Fig. 2. Temporal traces of conversions of the monomer-thiol mixtures at various mono-thiol concentrations.

Figure 3 shows parametric plots of relative conversion and R_p for the monomer-thiol mixtures at various mono-thiol concentrations. The relative conversion was defined as a time-dependent conversion normalized by the final conversion [28]. It can be seen that the maxima of R_p increase with increasing mono-thiol concentrations as a result of the chain-transfer process in the early period of free radical-mediated chain-growth polymerizations by the acrylate monomer. The rapid decrease in R_p after the gel point conversion (*i.e.*, the conversion point that gives the peak value of R_p) [12, 28] is caused by the rapid decrease in the number of propagating acrylate monomer-radical chains due to the termination by mono-thiols, resulting in a reduction of the crosslinking density. It can also be seen that the gel point conversion increases with increasing mono-thiol concentrations. It was reported that the delayed gel point conversion results in lowering the shrinkage in thiol-ene photopolymerizations [12]. Our

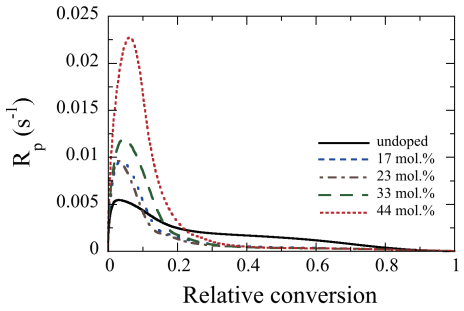

Fig. 3. R_p versus relative conversion for the monomer-thiol mixture at various mono-thiol concentrations.

observation suggests that mono-thiol doping can be used to reduce shrinkage due to the suppression of the rapid gelation in free radical-mediated chain-growth polymerizations [22]. This point will be also examined by the holographic shrinkage measurement described below.

Figure 4 shows a dependence of Δn_{sat} on molar concentrations of doped mono-thiols. It can be seen that there exists the optimum thiol concentration (∼33 mol.%) until which Δn_{sat} monotonically increases as large as 1.6×10^{-2}, two-fold enhancement of Δn_{sat} as compared to the undoped case. It also corresponds to two-fold enhancement of Δn_{neu} since it is proportional to Δn_{sat} as mentioned in the introduction. This result

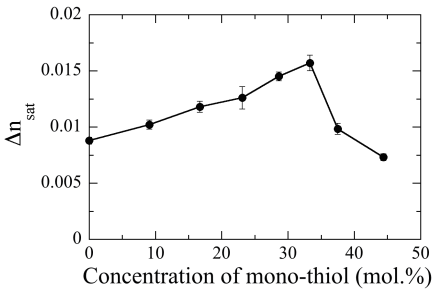

Fig. 4. Dependence of Δn_{sat} on molar concentration of mono-thiol. The grating spacing is 1 μm.

is attributed to the fact that thiol doping causes a decrease in the cross-linking density of the formed polymer and thereby the viscosity of the system. It also facilitates the mutual diffusion of nanoparticles and monomer. On the other hand, the rapid decrease in Δn_{sat} at higher thiol concentrations may be caused by the termination of primary radicals with excessive thiol radicals [24], thereby suppressing the polymerization of unreacted monomer.

Figure 5 shows a dependence of σ on molar concentrations of doped mono-thiols after holographic recording. It can be seen that shrinkage decreases with an increase in thiol concentration. The observed substantive reduction in σ by doping thiols is consistent with the result shown in Fig. 3 that predicts this trend. It can be attributed to the suppression of the rapid gelation in

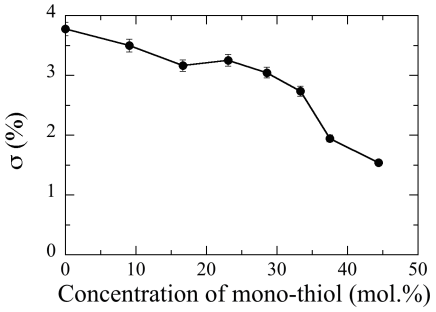

Fig. 5. Dependence of σ on molar concentration of mono-thiol. The grating spacing is 1 μm.

chain-growth polymerization by doping thiols.

Figure 6 shows a grating-spacing dependence of Δn_{sat}. It can be seen that the incorporation of mono-thiol increases Δn_{sat} at all the grating spacing used. The decreasing trend of Δn_{sat} with shortening grating spacing is typical for multi-component holographic photopolymers and is also caused by the non-local response [20]. The average polymer chain length shortens and the viscosity decreases because of the premature termination by doping thiols in free radical-mediated chain-growth polymerizations [24]. This chemical modification results in the improvement of the spatial frequency response, which is preferable for light and neutron optics applications with NPC volume gratings.

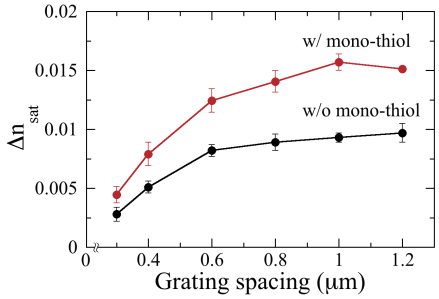

Fig. 6. Grating spacing dependence of Δn_{sat} without and with 33 mol.% mono-thiols.

In conclusion, we have demonstrated the enhancement of Δn_{sat} (and, therefore, of Δn_{neu}) in high spatial frequency regions and the suppression of polymerization shrinkage by incorporating chain-transferring mono-thiols in (meth)acrylate-based NPC films. Such simultaneous improvement is very useful for holographic applications in light and neutron optics. Similar improvement can be expected in SiO_2 nanoparticle-dispersed NPCs [5] exhibiting also good performance in slow-neutron optics [17–19]. In addition, since multi-functional thiols as chain-transfer agents can contribute to the modification of polymer network structures due to crosslinking through chain ends [25,29], it is expected that they alter the volume grating properties even more as compared to mono-thiols. Investigation of the effect of thiol doping on lifetime and stability of recorded NPC gratings are also of importance for the practicability of applications. Studies in these directions are currently underway.

One of the authors, J. Guo, acknowledges the financial support by JSPS KAKENHI grant number 25·03052.

References

1. R. A. Lessard and G. Manivannan, Proc. SPIE **2405**, 2 (1995).
2. L. Hesselink, S.S. Orlov, and M.C. Bashaw, Proc. IEEE **92**, 1231 (2004).
3. G. P. Crawford, Opt. & Photonics News, April, 54 (2003).
4. N. Suzuki, Y. Tomita, and T. Kojima, Appl. Phys. Lett. **81**, 4121 (2002).
5. N. Suzuki and Y. Tomita, Appl. Opt. **43**, 2125 (2004).
6. N. Suzuki, Y. Tomita, K. Ohmori, M. Hidaka, and K. Chikama, Opt. Express **14**, 12712 (2006).
7. O. V. Sakhno, L. M. Goldenberg, J. Stumpe, and T. N. Smirnova, Nanotechnology **18**, 105704 (2007).
8. O. V. Sakhno, T. N. Smirnova, L. M. Goldenberg, and J. Stumpe, Mater. Sci. Eng. C **28**, 28 (2008).
9. M. Moothanchery, I. Naydenova, S. Mintova, and V. Toal, Opt. Express **19**, 1339 (2011).
10. Y. Tomita, N. Suzuki, and K. Chikama, Opt. Lett. **30**, 839 (2005).
11. Y. Tomita, T. Nakamura, and A. Tago, Opt. Lett. **33**, 1750 (2008).
12. E. Hata, K. Mitsube, K. Momose, and Y. Tomita, Opt. Mater. Express **1**, 207 (2011).
13. K. Momose, S. Takayama, E. Hata, and Y. Tomita, Opt. Lett. **37**, 2250 (2012).
14. T. N. Smirnova, O. V. Sakho, P. V. Yezhov, L. M. Kokhtych, L. M. Goldenberg, and J. Stumpe, Nanotechnology **20**, 245707 (2009).
15. T. N. Smirnova, O. V. Sakho, J. Stumpe, V. Kzianzou, and S. Schrader, J. Opt **13**, 035709 (2011).
16. X. Liu, Y. Adachi, Y. Tomita, J. Oshima, T. Nakashima, and T. Kawai, Opt. Express **20**, 13457 (2012).
17. M. Fally, J. Klepp, Y. Tomita, T. Nakamura, C. Pruner, M. A. Ellaban, R.A. Rupp, M. Bichler, I. Drevenšek-Olenik, J. Kohlbrecher, H. Eckerlebe, H. Lemmel, and H. Rauch, Phys. Rev. Lett. **105**, 123904 (2010).
18. J. Klepp, C. Pruner, Y. Tomita, C. Plonka-Spehr, P. Geltenbort, S. Ivanov, G. Manzin, K. H. Andersen, J. Kohlbrecher, M. A. Ellaban, and M. Fally, Phys. Rev. A **84**, 013621 (2011).
19. J. Klepp, C. Pruner, Y. Tomita, K. Mitsube, P. Geltenbort, and M. Fally, Appl. Phys. Lett. **100**, 214104 (2012).
20. J. T. Sheridan and J. R. Lawrence, J. Opt. Soc. Am. A **17**, 1108 (2000).
21. S. Meng, T. Kyu, L. V. Natarajan, V. P. Tondiglia, R. L. Sutherland, and T. J. Bunning, Macromolecules **38**, 4844 (2005).
22. G. Odian, *Principles of Polymerization*, 4th ed. (Wiley, New York, 1994), Chap.3, p.238.
23. M. R. Gleeson, D. Sabol, S. Liu, C. E. Close, J. V. Kelly, and J. T. Sheridan, J. Opt. Soc. Am. B **25**, 396 (2008).
24. J. Guo, M. R. Gleeson, S. Liu, and J. T. Sheridan, J. Opt. **13**, 095602 (2011).
25. C. S. Pfeifer, N. D. Wilson, Z. R. Shelton, and J. W. Stansbury, Polymer **52**, 3295 (2011).
26. N. Uchida, J. Opt. Soc. Am. **63**, 280 (1973).
27. L. Dhar, M. G. Schones, T. L. Wysocki, H. Bair, M. Schilling, and C. Boyd, Appl. Phys. Lett. **73**, 1337 (1998).
28. T.-M. G. Chu and J. W. Halloran, J. Am. Ceram. Soc. **83**, 2375 (2000).
29. T. Y. Lee, J. Carioscia, Z. Smith, C. N. Bowman, Macromolecules **40**, 1473 (2007).

Informational Fourth Page

References

1. R. A. Lessard and G. Manivannan, "Holographic recording materials: an overview," Proc. SPIE **2405**, 2–23 (1995).
2. L. Hesselink, S.S. Orlov, and M.C. Bashaw, "Holographic data storage systems," Proc. IEEE **92**, 1231–1280 (2004).
3. G. P. Crawford, "'Electrically switchable Bragg gratings," Opt. & Photonics News, April, 54–59 (2003).
4. N. Suzuki, Y. Tomita, and T. Kojima, "Holographic recording in TiO_2 nanoparticle-dispersed methacrylate photopolymer films," Appl. Phys. Lett. **81**, 4121–4123 (2002).
5. N. Suzuki and Y. Tomita, "Silica-nanoparticle-dispersed methacrylate photopolymers with net diffraction efficiency near 100%," Appl. Opt. **43**, 2125–2129 (2004).
6. N. Suzuki, Y. Tomita, K. Ohmori, M. Hidaka, and K. Chikama, "Highly transparent ZrO_2 nanoparticle-dispersed acrylate photopolymers for volume holographic recording," Opt. Express **14**, 12712–12719 (2006).
7. O. V. Sakhno, L. M. Goldenberg, J. Stumpe, and T. N. Smirnova, "Surface modified ZrO_2 and TiO_2 nanoparticles embedded in organic photopolymers for highly effective and UV-stable volume holograms," Nanotechnology **18**, 105704 (2007).
8. O. V. Sakhno, T. N. Smirnova, L. M. Goldenberg, and J. Stumpe,"Holographic patterning of luminescent photopolymer nanocomposites," Mater. Sci. Eng. C **28**, 28–35 (2008).
9. M. Moothanchery, I. Naydenova, S. Mintova, and V. Toal, "Study of the shrinkage caused by holographic grating formation in acrylamide based photopolymer film," Opt. Express **19**, 13395–13404 (2011).
10. Y. Tomita, N. Suzuki, and K. Chikama, "Holographic manipulation of nanoparticle distribution morphology in nanoparticle-dispersed photopolymers," Opt. Lett. **30**, 839–841 (2005).
11. Y. Tomita, T. Nakamura, and A. Tago, "Improved thermal stability of volume holograms recorded in nanoparticle-polymer composite films," Opt. Lett. **33**, 1750–1752 (2008).
12. E. Hata, K. Mitsube, K. Momose, and Y. Tomita, "Holographic nanoparticle-polymer composites based on step-growth thiol-ene photopolymerization," Opt. Mater. Express **1**, 207–222 (2011).
13. K. Momose, S. Takayama, E. Hata, and Y. Tomita, "Shift-multiplexed holographic digital data page storage in a nanoparticle-(thiol-ene) polymer composite film," Opt. Lett. **37**, 2250–2252 (2012).
14. T. N. Smirnova, O. V. Sakho, P. V. Yezhov, L. M. Kokhtych, L. M. Goldenberg, and J. Stumpe, "Amplified spontaneous emission in polymer-CdSe/ZnS-nanocrystal DFB structures produced by the holographic method," Nanotechnology **20**, 245707 (2009).
15. T. N. Smirnova, O. V. Sakho, J. Stumpe, V. Kzianzou, and S. Schrader, Distributed feedback lasing in dye-doped nanocomposite holographic transmission gratings," J. Opt **13**, 035709 (2011).
16. X. Liu, Y. Adachi, Y. Tomita, J. Oshima, T. Nakashima, and T. Kawai, "High-order nonlinear optical response of a polymer nanocomposite film incorporating semiconducotor CdSe quantum dots," Opt. Express **20**, 13457–13469 (2012).
17. M. Fally, J. Klepp, Y. Tomita, T. Nakamura, C. Pruner, M. A. Ellaban, R.A. Rupp, M. Bichler, I. Drevenšek-Olenik, J. Kohlbrecher, H. Eckerlebe, H. Lemmel, and H. Rauch, "Neutron optical beam splitter from holographically structured nanoparticle-polymer composites," Phys. Rev. Lett. **105**, 123904 (2010).
18. J. Klepp, C. Pruner, Y. Tomita, C. Plonka-Spehr, P. Geltenbort, S. Ivanov, G. Manzin, K. H. Andersen, J. Kohlbrecher, M. A. Ellaban, and M. Fally, "Diffraction of slow neutrons by holographic SiO_2 nanoparticle-polymer composite gratings," Phys. Rev. A **84**, 013621 (2011).
19. J. Klepp, C. Pruner, Y. Tomita, K. Mitsube, P. Geltenbort, and M. Fally, "Mirrors for slow neutrons from holographic nanoparticle-polymer free-standing film-gratings," Appl. Phys. Lett. **100**, 214104 (2012).
20. J. T. Sheridan and J. R. Lawrence, "Nonlocal response diffusion model of holographic recording in photopolymer," J. Opt. Soc. Am. A **17**, 1108–1114 (2000).
21. S. Meng, T. Kyu, L. V. Natarajan, V. P. Tondiglia, R. L. Sutherland, and T. J. Bunning, "Holographic photopolymerization-induced phase separation in reference to the phase diagram of a mixture of photocurable monomer and nematic liquid crystal," Macromolecules **38**, 4844–4854 (2005).
22. G. Odian, *Principles of Polymerization*, 4th ed. (Wiley, New York, 1994), Chap.3, p.238.
23. M. R. Gleeson, D. Sabol, S. Liu, C. E. Close, J. V. Kelly, and J. T. Sheridan, "Improvement of the spatial frequency response of photopolymer materials by modifying polymer chain length," J. Opt. Soc. Am. B **25**, 396–406 (2008).
24. J. Guo, M. R. Gleeson, S. Liu, and J. T. Sheridan, "Nonlocal spatial frequency response of photopolymer materials containing chain transfer agents: Part II. Experimental results," J. Opt. **13**, 095602 (2011).
25. C. S. Pfeifer, N. D. Wilson, Z. R. Shelton, and J. W. Stansbury, "Delayed gelation through chain-transfer reactions: Mechanism for stress reduction in methacrylate networks," Polymer **52**, 3295–3303 (2011).
26. N. Uchida, "Calculation of diffraction efficiency in hologram gratings attenuated along the direction perpendicular to the grating vector," J. Opt. Soc. Am. **63**, 280–287 (1973).
27. L. Dhar, M. G. Schones, T. L. Wysocki, H. Bair, M. Schilling, and C. Boyd, "Temperature-induced changes in photopolymer volume holograms," Appl. Phys. Lett. **73**, 1337–1339 (1998).
28. T.-M. G. Chu and J. W. Halloran, "Curing of highly loaded ceramic suspensions in acrylates," J. Am. Ceram. Soc. **83**, 2375–2380 (2000).
29. T. Y. Lee, J. Carioscia, Z. Smith, C. N. Bowman, "Thiol-allyl ether-methacrylate ternary systems. Evolution mechanism of polymerization-induced shrinkage stress and mechanical properties," Macromolecules **40**, 1473–1479 (2007).